diversity

MDPI

Article

Identification and Characterization of UDP-Glycosyltransferase Genes in a Cerambycid Beetle, *Pharsalia antennata* Gahan, 1894 (Coleoptera: Cerambycidae)

Ningna Yin, Zhengquan Wang, Haiyan Xiao, Tingting Lu and Naiyong Liu *

Key Laboratory of Forest Disaster Warning and Control of Yunnan Province, Southwest Forestry University, Kunming 650224, China; yinningna@swfu.edu.cn (N.Y.); wzq15198369955@swfu.edu.cn (Z.W.); xiaohaiyan@swfu.edu.cn (H.X.); lutingting@swfu.edu.cn (T.L.)
* Correspondence: naiyong_2013@163.com; Tel./Fax: +86-871-63862665

Abstract: The cerambycid beetle, *Pharsalia antennata* Gahan, 1894 (Coleoptera: Cerambycidae), is a wood-boring pest that spends most of its life cycle in the trunks or under the bark of trees. These distinctive biological characteristics make it likely that this beetle will encounter a number of plant defensive compounds, coupled with a broad range of host plants, possibly resulting in the overexpression or expansion of uridine diphosphate (UDP)-glycosyltransferase (UGT) genes. Here, we identified and characterized the UGT gene family in *P. antennata* through transcriptome data, sequence and phylogenetic analyses, and PCR and homology modeling approaches. In total, 59 transcripts encoding UGTs were identified, 34 of which harbored full-length sequences and shared high conservation with the UGTs of *Anoplophora glabripennis*. Of the 34 PantUGTs, only 31.78% amino acid identity was observed on average, but catalytic and sugar binding residues were highly conserved. Phylogenetic analyses revealed four Cerambycidae-specific clades, including 30 members from *P. antennata*. Combining the transcriptome and PCR data showed that PantUGTs had a wide tissue expression, and the majority of the genes were presented mainly in antennae or abdomens, suggesting their putative roles in olfaction and detoxification. This study provides, for the first time, information on the molecular and genetic basis of *P. antennata*, greatly enhancing our knowledge of the detoxification-related UGT gene family.

Keywords: *Pharsalia antennata*; UDP-glycosyltransferase; phylogenetic analysis; expression profile; olfaction

Citation: Yin, N.; Wang, Z.; Xiao, H.; Lu, T.; Liu, N. Identification and Characterization of UDP-Glycosyltransferase Genes in a Cerambycid Beetle, *Pharsalia antennata* Gahan, 1894 (Coleoptera: Cerambycidae). *Diversity* **2022**, *14*, 348. https://doi.org/10.3390/d14050348

Academic Editors: Roberto Pizzolotto, Amit Roy and Audrey Bras

Received: 29 March 2022
Accepted: 27 April 2022
Published: 28 April 2022

1. Introduction

Cerambycidae spend most of their life cycle in the trunks or under the bark of trees, and so they are likely to encounter many plant-derived allelochemicals. As an evolutionary adaptation of the insects to the host plants, they must positively respond to these toxic chemicals and develop a sophisticated detoxification enzyme system to degrade these substrates [1–4]. The uridine diphosphate (UDP)-glycosyltransferase (UGT) gene family is one of the most important detoxification enzyme gene families, and it can catalyze hydroxyl compounds with glucose into hydrophilic molecules that are easily excreted. As well as being found in insects, UGTs are also presented extensively in other animals, plants and microbes [5–7].

Like human UGTs, insect UGTs are composed of a diverse N-terminus and a conserved C-terminus, in which the latter contains sugar donor binding regions (DBRs) and key residues, and thus is responsible for detoxification, olfaction, pigmentation and insecticide resistance [8,9]. In *Bombyx mori* Linnaeus, 1758 (Lepidoptera: Bombycidae), UGTs are capable of catalyzing the glycosylation of lipophilic xenobiotics, including flavonoids and terpenoids [10,11]. In the three noctuid moths *Helicoverpa armigera* Hübner, 1808 (Lepidoptera: Noctuidae), *Heliothis virescens* Fabricius, 1777 (Lepidoptera: Noctuidae) and *Spodoptera frugiperda* Smith, 1797

(Lepidoptera: Noctuidae), host-plant-derived toxic chemicals can be detoxified by UGT enzymes, highlighting their roles in the adaptation of herbivorous insects to hosts [12,13]. Regarding the specific or high expression of UGT genes in antennae, it is suggested that they may participate in the sensing of odorants [14–19]. Typically, the UGT enzymes are associated with insecticide resistance, as observed in *Aphis gossypii* Glover, 1877 (Hemiptera: Aphididae) [20,21], *Bemisia tabaci* Gennadius, 1889 (Hemiptera: Aleyrodidae) [22], *Diaphorina citri* Kuwayama, 1907 (Hemiptera: Chermidae) [23], *Anopheles sinensis* Wiedemann, 1828 (Diptera: Culicidae) [24], *Drosophila melanogaster* Meigen, 1830 (Diptera: Drosophilidae) [25], *Anopheles gambiae* Giles, 1900 (Diptera: Culicidae) [26] and *Plutella xylostella* Linnaeus, 1758 (Lepidoptera: Plutellidae) [27]. However, coleopteran UGTs have received little attention, especially regarding their functions. Based on genome and transcriptome data, there are 65, 43, 36, 30, 20 and 8 UGT relatives in *Anoplophora glabripennis* Motschulsky, 1853 (Coleoptera: Cerambycidae) [28], *Tribolium castaneum* Herbst, 1797 (Coleoptera: Tenibroidae) [8], *Rhaphuma horsfieldi* White, 1855 (Coleoptera: Cerambycidae) [29], *Xylotrechus quadripes* Chevrolat, 1863 (Coleoptera: Cerambycidae) [14], *Holotrichia parallela* Motschulsky, 1854 (Coleoptera: Scarabaeidae) [15] and *Phyllotreta striolata* Fabricius, 1803 (Coleoptera: Chrysomelidae) [30], respectively. In *Leptinotarsa decemlineata* Say, 1824 (Coleoptera: Chrysomelidae), LdecUGT2 is involved in imidacloprid resistance [31].

The cerambycid beetle, *Pharsalia antennata* Gahan, 1894 (Coleoptera: Cerambycidae), is a destructive wood borer with its larvae feeding mainly on the Juglandaceae plants. In 2019, we first reported its new host plant, *Juglans sigillata* Dode, 1906 (Juglandales: Julandaceae), in Yunnan Province in China. This species is also distributed in Guangxi, Fujian and Hunan in China, as well as in India, Myanmar and Laos [32]. To date, very little is known about its biology and physiology, especially the genetic and molecular basis underlying the interactions between this species and hosts or the external environment. Prior to this study, the sensilla of two crucial chemosensory organs (i.e., antennae and tarsi) from *P. antennata* were characterized [32]. To enhance our knowledge of the detoxification mechanisms in this pest, in this study we characterized the UGT gene family of *P. antennata* through gene identification, sequence and phylogenetic analyses, and expression characteristics. This study complements information on the detoxification genes in *P. antennata* and identifies candidate molecular targets associated with olfaction, gustation or detoxification.

2. Materials and Methods

2.1. Insect Rearing and Tissue Collection

The pupae of *P. antennata* were collected from Santai Village, Dayao County, Chuxiong City, Yunnan Province, China (26°00′01.6″ N, 101°04′04.7″ E) at an altitude of 1999 m. In brief, the damaged trunks of *J. sigillata* with oviposition scars were brought to the laboratory and kept at room temperature. The wounds in the tree trunks were painted using Vaseline and then wrapped with Parafilm. The emerged adults were sexed [32] and kept separately in individual cages with 10% honey solution, leaves and wood walnuts. Various tissues were collected from 3- to 5-day-old females and males, including 10 antennae, 10 heads without antennae, 3 thoraxes, 2 abdomens, 20 legs and 30 wings for each sex. All collected tissues were immediately frozen in liquid nitrogen and stored at −80 °C until use.

2.2. RNA Isolation and cDNA Synthesis

Total RNA was extracted from each tissue using TRIzol Reagent (Ambion, Life Technologies, Carlsbad, CA, USA), following the manufacturer's instructions. The concentration and quality of RNA were measured with a NanoDrop 1000 spectrophotometer (Thermo Fisher Scientific, San Jose, CA, USA). First-stranded cDNA was synthesized using 1 μg of total RNA and a PrimeScript RT Reagent Kit (TaKaRa, Dalian, China). The cDNA templates were stored at −20 °C and used for the subsequent expression profiling analyses of the genes.

2.3. Gene Identification

Based on the sequenced transcriptome data of *P. antennata* (Sequence Read Archive (SRA) accession numbers SRX14711840–SRX14711851), candidate genes encoding UGTs were identified using a BLAST-based homology method in the BioEdit v7.0.9.1 software (Ibis BioSciences, Carlsbad, CA, USA) [33], with the UGT queries from *A. glabripennis* [28], *R. horsfieldi* [29], *X. quadripes* [14] and *T. castaneum* [8]. Open reading frames (ORFs) of genes were predicted by the National Center for Biotechnology Information (NCBI) ORF Finder (https://www.ncbi.nlm.nih.gov/orffinder/ (accessed on 3 December 2021). All identified UGT genes were verified against the NCBI non-redundant (nr) protein sequence database using BLASTP.

2.4. Sequence Analysis

The identities of amino acid sequences of UGTs were calculated using GeneDoc v2.7.0.0 (Free Software Foundation Inc., Boston, MA, USA) [34]. The signal peptides of UGTs were predicted using the SignalP 6.0 server (https://services.healthtech.dtu.dk/service.php?SignalP-6.0 (accessed on 5 February 2022)) [35]. The theoretical isoelectric point (*p*I) and molecular weight (Mw) were computed using Compute *p*I/Mw (https://web.expasy.org/compute_pi/ (accessed on 5 December 2021)). The identification of *N*-glycosylation predicted sites (NPS) was performed using the NetNGlyc 1.0 server (http://www.cbs.dtu.dk/services/NetNGlyc/ (accessed on 5 December 2021)). Multiple alignments of amino acid sequences were performed using MAFFT v7.450 (Genome Resource and Analysis Unit, Kobe, Hyogo, Japan) [36].

2.5. Phylogenetic Tree Construction

In the phylogenetic analysis, UGT sequences from *P. antennata* and 14 other coleopteran species were selected. Of these, the UGTs with fewer than 100 amino acids were discarded. The amino acid sequences were aligned using MAFFT v7.450 [36]. A phylogenetic tree was constructed using FastTree v2.1.11 (Lawrence Berkeley National Lab, Berkeley, California, USA) with SH-like 1000 support [37]. The tree was edited and viewed using FigTree v1.4.3 (University of Edinburgh, Edinburgh, UK) (http://tree.bio.ed.ac.uk/software/figtree/ (accessed on 2 March 2022)). All the sequences used in the tree are shown in the Supplementary Material (Additional File S1).

2.6. Expression Profiling Analysis

In the expression profiles, the expression levels of genes in various tissues were first computed using FPKM (expected number of fragments per kilobase of transcript per millions of base pairs sequenced) values [38]. Based on the FPKM results, we further selected 32 UGT genes from *P. antennata* to validate their expression with reverse transcription PCR (RT–PCR) assays. These selected genes had specific or high expression in antennae, thoraxes or abdomens of both sexes. A reference gene, ribosomal protein S3 (PantRPS3), was used to check the quality and quantity of cDNA templates. Gene-specific primers (Table S1) were designed by Primer Premier 5.0 (PREMIER Biosoft International, Palo Alto, CA, USA), with the following parameters: GC contents of 45–55%, T_m values of 60 ± 1 °C and PCR product sizes of 400–500 bp. PCR reactions were performed, according to the instructions of a Taq DNA Polymerase kit (TaKaRa, Dalian, China), at 94 °C for 3 min, followed by 35 cycles at 94 °C for 30 s, 60 °C for 30 s, 72 °C for 40 s and a final extension at 72 °C for 5 min. The amplification products were detected and analyzed using 1.2% (*w*/*v*) agarose gels.

To address the putative roles of UGT genes in olfaction, 34 UGT genes with full-length ORFs were selected in quantitative real-time PCR (qPCR) analyses. The primers (Table S1) were designed by Beacon Designer 8.14 (PREMIER Biosoft International, Palo Alto, CA, USA). The reaction procedures were as follows: initial denaturation at 95 °C for 2 min, followed by 40 cycles at 95 °C for 10 s, 58 °C for 31 s and 72 °C for 30 s. Three biological replicates were performed, with three technical replicates for each template. Two reference

genes, ribosomal protein L10 (PantRPL10) and PantRPS3, were used to calculate the relative expression levels of target genes using the Q-Gene method [39,40]. Significant differences in the data were analyzed using Student's *t*-test, implemented in GraphPad Prism 7.00 (GraphPad Software Inc., San Diego, CA, USA).

2.7. Homology Modeling of P. antennata UGT2

Based on the crystal structure and related protein sequence of HsapUGT2B7 (PDB: 2O6L) from *Homo sapiens* Linnaeus, 1758 (Primates: Hominidae) [41], amino acid sequences of HsapUGT2B7 and 34 PantUGTs were aligned. PantUGT2 showed the highest identity with HsapUGT2B7 (41.18%) and was selected for construction of its tertiary structure. Homology modeling was conducted using SWISS-MODEL [42]. The structure was edited and visualized with PyMOL v1.7.2.1 (DeLano Scientific LLC, South San Francisco, CA, USA) (https://pymol.org/ (accessed on 2 March 2022)).

3. Results

3.1. Identification of Candidate UGT Genes in P. antennata

Transcriptome analyses led to the identification of 59 transcripts encoding UGTs in *P. antennata*, 34 of which were predicted to have full-length ORFs. These full-length sequences encoded 499 to 533 amino acids and had signal peptides (17–27 amino acids). The Mw and *p*I values of 34 PantUGTs were 56.98–61.38 kDa and 6.14–9.44, respectively. Most of the full-length UGTs (25/34) harbored over two *N*-glycosylation predicted sites, of which five relatives (PantUGT7, UGT10, UGT13, UGT14 and UGT23) presented six sites. In the BLAST searches of PantUGTs, except for PantUGT29 and AglaUGT2B31 (accession number: XP_018561622.1) (46%) in *A. glabripennis*, the PantUGTs shared over 50% amino acid identities with AglaUGTs, with some pairs exhibiting particularly high conservation (>90% identities). The remaining 25 PantUGTs were partial sequences with sizes of 136–524 amino acids. Most of the genes (21/25) also showed relatively high identities (>60%) with AglaUGTs (Table 1 and Supplementary Material Additional File S1).

Table 1. The information for candidate PantUGT genes of *P. antennata*.

Gene	ORF (AA)	Full Length	Signal Peptide (AA)	*p*I/Mw (kDa)	NPS	NCBI Blast Hit to *Anoplophora glabripennis* (Reference/Name)	*E* Value	Identity (%)
UGT1	517	Yes	20	8.88/58.57	129 | 174 | 239 | 509	XP_018579880.1 UDP-glucuronosyltransferase 2B10	0.0	83
UGT2	517	Yes	18	8.93/58.86	107 | 415 | 416 | 452	XP_023312103.1 UDP-glucuronosyltransferase 2B15	0.0	79
UGT3	517	Yes	18	8.79/59.32	65 | 121 | 220 | 397	XP_018561507.1 UDP-glucuronosyltransferase 2B7	0.0	68
UGT4	520	Yes	18	7.05/59.53	64 | 233	XP_018563298.1 UDP-glucuronosyltransferase 2B10	0.0	87
UGT5	512	Yes	18	8.70/58.16	120 | 230 | 456	XP_018563256.1 UDP-glucuronosyltransferase 2B7-like	0.0	84
UGT6	516	Yes	22	8.96/58.92	119 | 175 | 240	XP_018579878.1 UDP-glucuronosyltransferase 2B31	0.0	83
UGT7	519	Yes	19	9.24/59.03	66 | 81 | 88 | 222 | 232 | 419	XP_018561504.1 UDP-glucuronosyltransferase 2B37 isoform X1	0.0	56
UGT8	526	Yes	27	9.14/61.25	91 | 246 | 429 | 517	XP_018561622.1 UDP-glucuronosyltransferase 2B31	0.0	85
UGT9	512	Yes	17	8.82/58.39	233 | 278 | 323	XP_018570348.1 UDP-glucuronosyltransferase 1-8	0.0	81
UGT10	523	Yes	19	8.73/58.99	50 | 94 | 128 | 173 | 238 | 273	XP_018579876.1 UDP-glucuronosyltransferase 2B15	0.0	76
UGT11	514	Yes	17	9.21/58.27	63 | 235	XP_018579879.1 UDP-glucuronosyltransferase 1-8	0.0	84
UGT12	523	Yes	18	8.29/60.04	226 | 517	XP_018564526.1 UDP-glucuronosyltransferase 2B13-like	0.0	91
UGT13	533	Yes	22	9.09/61.38	69 | 177 | 243 | 274 | 334 | 419	XP_018568770.1 UDP-glucuronosyltransferase 2B19 isoform X1	0.0	79
UGT14	499	Yes	20	7.36/56.98	66 | 169 | 234 | 302 | 417 | 461	XP_018565808.1 UDP-glucuronosyltransferase 2B16-like isoform X1	0.0	70

Table 1. *Cont.*

Gene	ORF (AA)	Full Length	Signal Peptide (AA)	*p*I/Mw (kDa)	NPS	NCBI Blast Hit to *Anoplophora glabripennis* (Reference/Name)	*E* Value	Identity (%)
UGT15	518	Yes	18	8.96/59.06	65	XP_018573571.1 UDP-glucuronosyltransferase 2B7-like	0.0	71
UGT16	515	Yes	20	9.28/59.34	170 | 235 | 409	XP_018563264.1 UDP-glucuronosyltransferase 2B37	0.0	73
UGT17	516	Yes	17	8.91/58.43	64 | 120 | 219	XP_018561507.1 UDP-glucuronosyltransferase 2B7	0.0	66
UGT18	517	Yes	18	8.95/58.41	49 | 62 | 65 | 72 | 121	XP_018561507.1 UDP-glucuronosyltransferase 2B7	0.0	67
UGT19	522	Yes	17	9.19/59.78	64 | 225	XP_018573569.1 UDP-glucuronosyltransferase 2B7	0.0	95
UGT20	527	Yes	19	9.41/59.13	101 | 171 | 188 | 197 | 236	XP_018562714.1 UDP-glucuronosyltransferase	0.0	73
UGT21	516	Yes	18	9.14/58.71	109 | 127 | 172 | 189 | 237	XP_018579881.1 UDP-glucuronosyltransferase 2B7-like	0.0	81
UGT22	514	Yes	17	8.95/59.13	48 | 119 | 229 | 289 | 455	XP_018562715.1 UDP-glucuronosyltransferase 2A3 isoform X1	0.0	84
UGT23	522	Yes	20	6.44/60.65	64 | 85 | 173 | 285 | 336 | 424	XP_018566903.1 UDP-glucuronosyltransferase 2B15-like	0.0	79
UGT24	527	Yes	21	8.65/59.92	52 | 82 | 239	XP_018561400.1 UDP-glucuronosyltransferase 2C1-like	0.0	96
UGT25	517	Yes	18	9.01/59.23	65 | 122 | 236	XP_018572801.1 UDP-glucuronosyltransferase 2B7	0.0	91
UGT26	516	Yes	19	8.42/59.11	50 | 457	XP_018570251.1 UDP-glucuronosyltransferase 1-6-like	0.0	74
UGT27	523	Yes	29	9.15/59.91	2 | 12 | 131 | 241 | 508	XP_018563266.1 UDP-glucuronosyltransferase 2B1	0.0	79
UGT28	511	Yes	17	6.58/58.41	64 | 166	XP_018561499.1 UDP-glucuronosyltransferase 2B7-like	0.0	70
UGT29	521	Yes	19	6.14/59.21	65 | 123 | 238 | 245 | 465	XP_018561622.1 UDP-glucuronosyltransferase 2B31	2×10^{-163}	46
UGT30	521	Yes	20	6.35/59.69	127 | 408	XP_018561584.1 uncharacterized protein LOC108903775	0.0	78
UGT31	520	Yes	20	7.63/58.90	51	XP_018569262.1 UDP-glucuronosyltransferase 2B7	0.0	77
UGT32	515	Yes	20	9.44/58.56	14 | 106 | 236 | 281 | 326	XP_018570347.1 UDP-glucuronosyltransferase 1-1 isoform X2	0.0	87
UGT33	521	Yes	24	9.24/58.90	112 | 176 | 242 | 287 | 332	XP_018570346.1 UDP-glucuronosyltransferase 1-3 isoform X1	0.0	87
UGT34	519	Yes	20	9.03/59.13	66 | 73 | 148 | 169 | 211	XP_023310147.1 UDP-glucuronosyltransferase 2B16-like isoform X1	0.0	80
UGT35	524	No				XP_018579876.1 UDP-glucuronosyltransferase 2B15	0.0	67
UGT36	522	No				XP_018561504.1 UDP-glucuronosyltransferase 2B37 isoform X1	0.0	77
UGT37	466	No				XP_018565808.1 UDP-glucuronosyltransferase 2B16-like isoform X1	0.0	75
UGT38	341	No				XP_018563264.1 UDP-glucuronosyltransferase 2B37	2×10^{-174}	70
UGT39	338	No				XP_018561507.1 UDP-glucuronosyltransferase 2B7	3×10^{-150}	65
UGT40	340	No				XP_018568773.2 UDP-glucuronosyltransferase 2B9	3×10^{-175}	73
UGT41	292	No				XP_018561504.1 UDP-glucuronosyltransferase 2B37 isoform X1	5×10^{-152}	73
UGT42	230	No				XP_018563273.1 UDP-glucuronosyltransferase 2B9-like	3×10^{-144}	86
UGT43	250	No				XP_018579876.1 UDP-glucuronosyltransferase 2B15	9×10^{-128}	76
UGT44	448	No				XP_018563300.1 UDP-glucuronosyltransferase 2B33-like	0.0	81
UGT45	275	No				XP_018579881.1 UDP-glucuronosyltransferase 2B7-like	1×10^{-153}	76
UGT46	413	No				XP_018563264.1 UDP-glucuronosyltransferase 2B37	0.0	77
UGT47	228	No				XP_018561584.1 uncharacterized protein LOC108903775	2×10^{-121}	78
UGT48	428	No				XP_023310231.1 UDP-glucuronosyltransferase 2B33-like	0.0	71
UGT49	453	No				XP_018579876.1 UDP-glucuronosyltransferase 2B15	0.0	82

Table 1. *Cont.*

Gene	ORF (AA)	Full Length	Signal Peptide (AA)	*p*I/Mw (kDa)	NPS	NCBI Blast Hit to *Anoplophora glabripennis* (Reference/Name)	*E* Value	Identity (%)
UGT50	436	No				XP_018579876.1 UDP-glucuronosyltransferase 2B15	0.0	79
UGT51	350	No				XP_018561520.1 UDP-glucuronosyltransferase 2B7-like	0.0	83
UGT52	287	No				XP_018570348.1 UDP-glucuronosyltransferase 1-8	9×10^{-139}	72
UGT53	316	No				XP_018563264.1 UDP-glucuronosyltransferase 2B37	0.0	89
UGT54	276	No				XP_018561499.1 UDP-glucuronosyltransferase 2B7-like	1×10^{-84}	49
UGT55	221	No				XP_018568773.2 UDP-glucuronosyltransferase 2B9	5×10^{-111}	73
UGT56	169	No				XP_018561622.1 UDP-glucuronosyltransferase 2B31	6×10^{-30}	39
UGT57	177	No				XP_018570251.1 UDP-glucuronosyltransferase 1-6-like	7×10^{-77}	65
UGT58	164	No				XP_018561504.1 UDP-glucuronosyltransferase 2B37 isoform X1	3×10^{-45}	53
UGT59	136	No				XP_018561622.1 UDP-glucuronosyltransferase 2B31	8×10^{-45}	52

AA: amino acid; ORF: open reading frame; Mw: molecular weight; NPS: *N*-glycosylation predicted site; *p*I: isoelectric point.

3.2. Sequence Characteristics of P. antennata UGTs

To identify key amino acids of 34 PantUGTs involved in sugar donor binding and conserved functional domains, their protein sequences were aligned and analyzed. The results showed that PantUGTs had an average of only 31.78% amino acid identity with each other, and PantUGT32 and PantUGT33 shared the highest identity of 79.42%, while the lowest was between PantUGT3 and PantUGT26 (24.14%). The C-terminal domain was more conserved than the N-terminal domain, especially for two DBRs (DBR1 and DBR2). In the N-terminal domain, two catalytic residues were highly conserved where the first site was histidine (H)/glutamine (Q)/asparagine (N) and the second was aspartic acid (D). In the C-terminal domain, the residues interacting with the sugar donor were also highly conserved, including nucleotide (serine/cysteine, S/C; tryptophan/phenylalanine, W/F; Q), phosphate (threonine/serine/tyrosine/methionine, T/S/Y/M; H/Q) and glycoside (D; glutamine/histidine/glutamic acid, Q/H/E) interacting residues. In addition, a signature motif, a transmembrane domain and a cytoplasmic tail were observed (Figure 1A).

Based on the crystal structure and amino acid sequence of HsapUGT2B7 in *H. sapiens* [41], the secondary structures of 34 PantUGTs were predicted and analyzed. The seven α-helixes had low amino acid identities, except for α3. The β-sheets shared relatively high conservation, including β1, β2 and β4. The key residues involved in sugar donor binding were highly conserved between HsapUGT2B7 and PantUGTs, i.e., S, W, Q and E for nucleotide interacting residues, T and H for phosphate interacting residues and D and Q for glycoside interacting residues (Figure 1A). There were identical residues in key sugar-donor binding sites between PantUGT2 and HsapUGT2B7. These conserved residues were positioned within the binding pocket of PantUGT2. In the superimposition of PantUGT2 and HsapUGT2B7 structures, four highly conserved regions (α3, β1, β2 and β4) constituted most of the binding pockets of UDP-glucose (UDPG). Compared to the structure of HsapUGT2B7, PantUGT2 had a shorter N-terminus, as well as more diverse loops (Figure 1B).

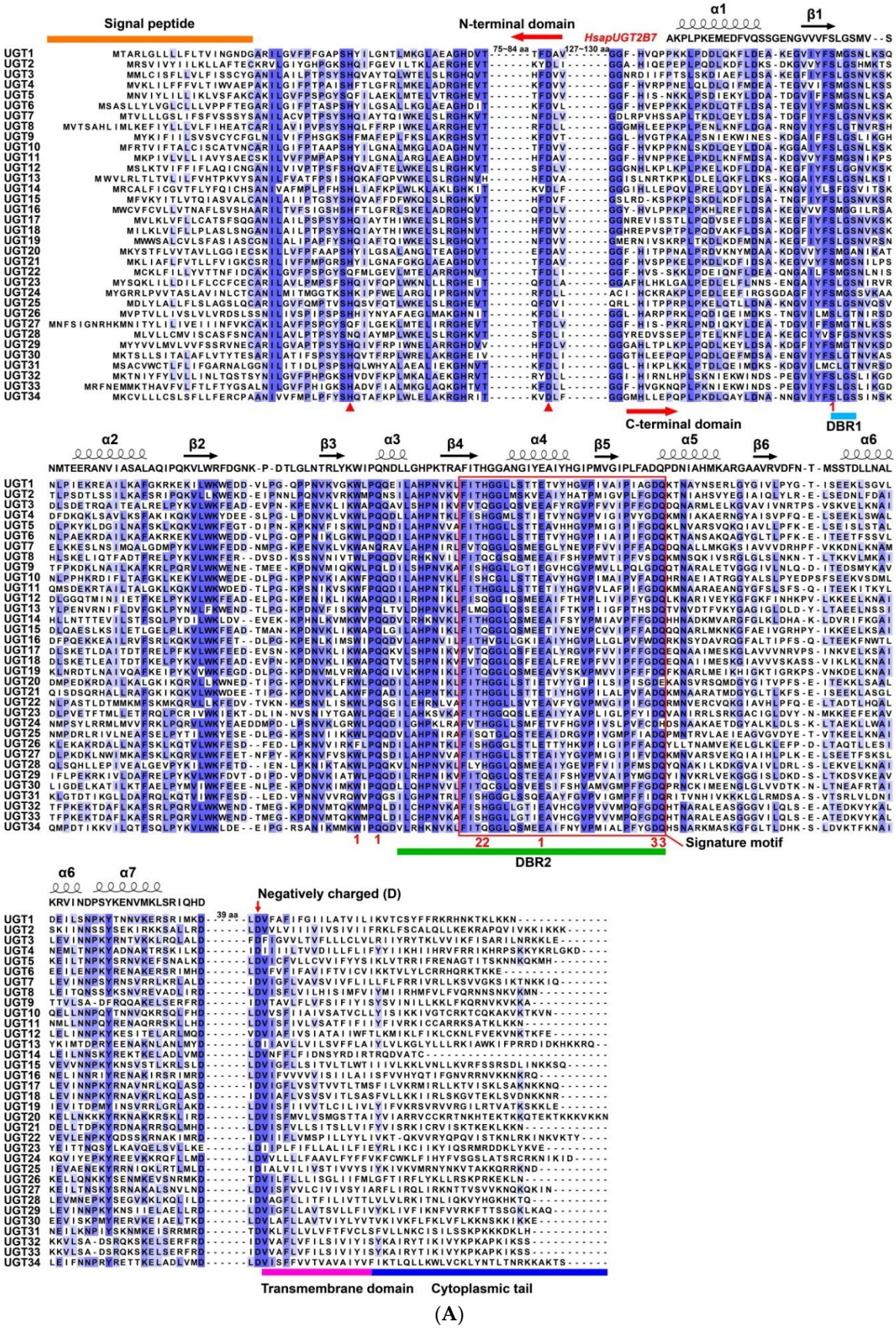

(**A**)

Figure 1. *Cont.*

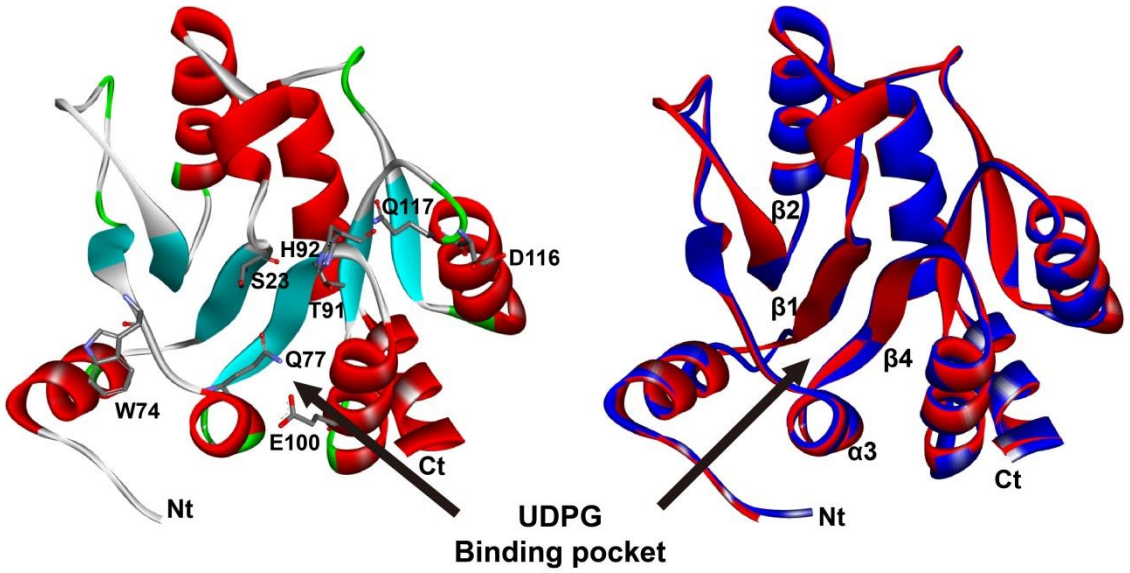

(**B**)

Figure 1. The UGT gene family in *P. antennata*. (**A**) Multiple alignments of amino acid sequences of 34 full-length PantUGTs. The signal peptides (orange), two donor binding regions (DBR1, cyan and DBR2, green), a transmembrane domain (magenta) and a cytoplasmic tail (blue) are indicated in colored boxes. Several key amino acids of DBRs involved in the sugar donor are shown by red numbers, including nucleotide interacting residues (1), phosphate interacting residues (2) and glucoside interacting residues (3). Two key catalytic residues (H and D) are labeled in red triangles. Other conserved amino acids with at least 30% identities in the sequences are shaded with a light-blue to dark-blue background. Based on the secondary structure of *H. sapiens* UGT2B7, α-helixes and β-sheets are indicated on the top of the alignment of PantUGTs. (**B**) The tertiary structure of PantUGT2 (**left**) and structural superimposition of PantUGT2 (red) and HsapUGT2B7 (blue) (**right**). Key residues (S23, W74, Q77, T91, H92, E100, D116 and Q117) and conserved regions (α3, β1, β2 and β4) are labeled on the structures. Arrows indicate the binding pockets of UDPG. Nt: N-terminus; Ct: C-terminus.

3.3. Phylogenetic Analysis of Coleopteran UGTs

In the phylogenetic analysis, a total of 576 UGT sequences of 15 coleopteran species, including the four cerambycid beetles *A. glabripennis*, *P. antennata*, *R. horsfieldi* and *X. quadripes*, were selected to construct the tree. The results revealed that coleopteran UGTs could be divided into 11 phylogenetic clades: UGT50, UGT311, UGT312, UGT319/320/321, UGT323, UGT324, UGT325, UGT328, UGT326/327/347, UGT331 and UGT352, where UGT319/320/321 and UGT326/327/347 were composed of mixed members. Some species- or family-specific expansions were found in the tree. For example, members of four clades were unique to the cerambycid beetles, including one in UGT323, one in UGT352 and two in UGT324. A similar lineage-specific expansion was also observed in the family Chrysomelidae. Several typical species-specific representatives were presented in *Nicrophorus vespilloides* Herbst, 1783 (Coleoptera: Silphidae) (13 UGTs in UGT319/320/321), *Agrilus planipennis* Fairmaire, 1888 (Coleoptera: Buprestidae) (10 UGTs in UGT319/320/321), *Aethina tumida* Murray, 1867 (Coleoptera: Nitidulidae) (9 UGTs in UGT312), *T. castaneum* (8 UGTs in UGT324) and *Onthophagus taurus* Schreber, 1759 (Coleoptera: Scarabaeidae) (8 UGTs in UGT311) (Figure 2).

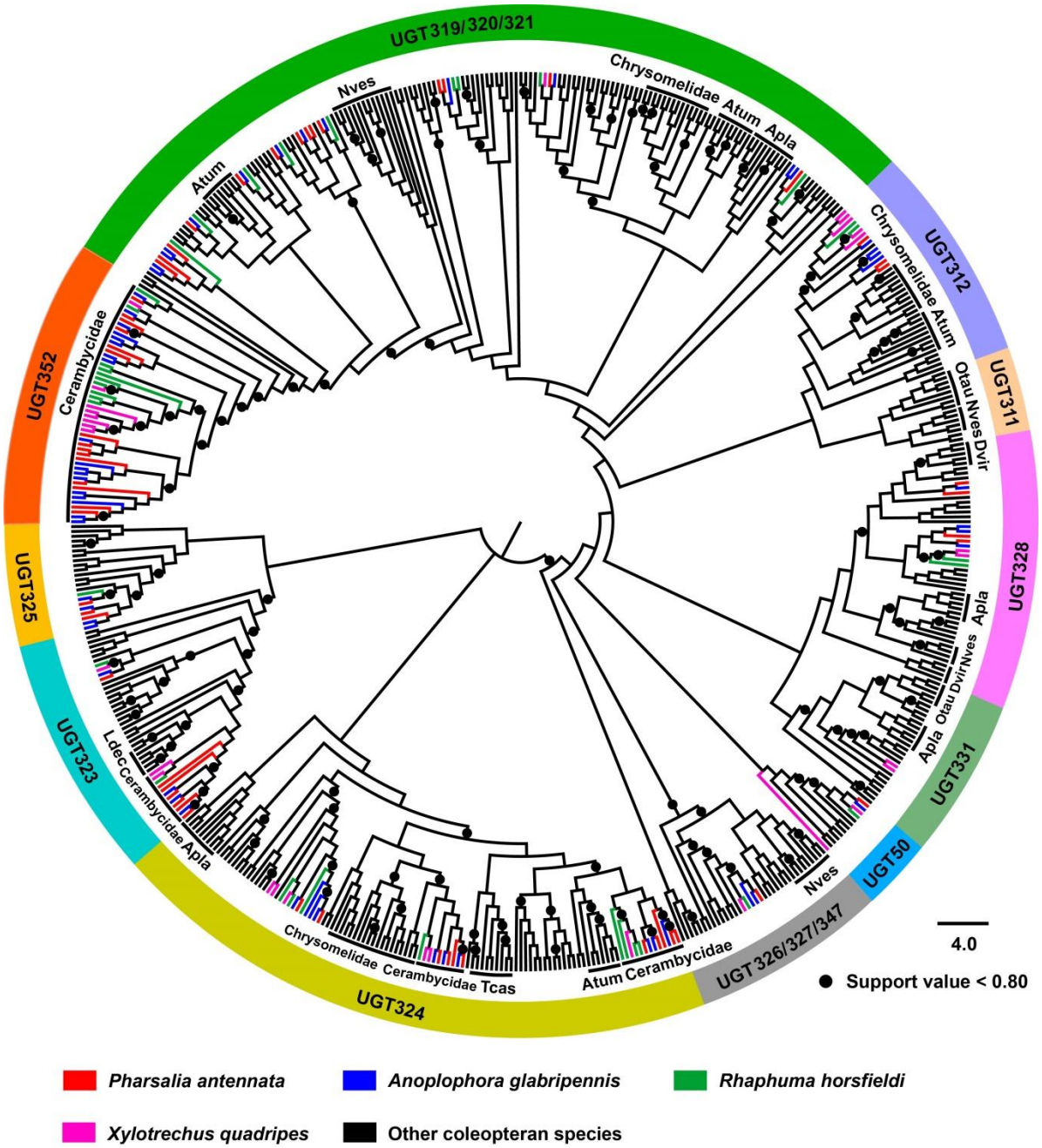

Figure 2. Phylogenetic relationship of coleopteran UGTs. The tree was constructed by FastTree v2.1.11, based on an aligned protein sequence of UGTs in 15 coleopteran species. Support values were computed with SH-like 1000 support. Species-specific color patterns of UGTs are presented for four cerambycid species, and the UGTs of other species are highlighted in black. Atum: *Aethina tumida*; Apla: *Agrilus planipennis*; Dvir: *Diabrotica virgifera virgifera*; Ldec: *Leptinotarsa decemlineata*; Nves: *Nicrophorus vespilloides*; Otau: emphOnthophagus taurus, Tcas: *Tribolium castaneum*.

Apart from the two clades UGT311 and UGT331, the nine clades possessed at least one member of PantUGTs in *P. antennata*. Of these, UGT352 was specific to the Cerambycidae and had 15 *P. antennata* UGTs, representing the most relatives among the nine clades. Both UGT319/320/321 and UGT324 harbored comparable gene numbers, with 14 and 11 relatives, respectively. A highly conserved UGT50 subfamily was composed of one singleton from each species, including *P. antennata*, in which 11 full-length UGT50 orthologs shared an average 72.88% amino acid identity with particularly high conservation (86.85%

identity) among four cerambycid species. In most cases, *P. antennata* UGTs clustered together with those in *A. glabripennis*, with 1:1 orthology (Figure 2).

3.4. Sex- and Tissue-Specific Expression Profile of P. antennata UGTs

Based on the FPKM values, an expression profiling map of 58 PantUGTs was constructed. Due to the existence of PantUGT58 only in the transcript database, the FPKM values in various tissues were unavailable. The majority of PantUGTs were highly expressed in thoraxes and/or abdomens of both sexes, for example PantUGT11, expressed in thoraxes (FPKM = 62.53 and 90.80 in males and females, respectively) and abdomens (FPKM = 52.02 in males and 96.61 in females), as well as PantUGT35 expressed in female abdomens (FPKM = 77.21). Eight of the 58 PantUGTs were detected in tissues at an extremely low level (FPKM < 2.00), including PantUGT3/5/8/23/41/45/54/57. Some genes exhibited comparable transcriptional levels in female and male antennae (FPKM > 20), including PantUGT16, UGT18 and UGT31. PantUGT38 showed 182-fold higher expression in males (FPKM = 43.77) than in females (FPKM = 0.24) (Figure 3A). Considering the abundant expression of 32 PantUGTs in thoraxes and/or abdomens, PCR was employed to validate their existence in 12 tissues. As expected, the expression of the genes was thorax- and/or abdomen-enriched, although most of them were also transcribed in other tissues. Eight genes had antenna-dominant expression, including PantUGT6/11/21/24/28/35/37/43 (Figure 3B).

Using qPCR assays, we further detected the relative expression of 34 candidate *UGT* genes in antennae and abdomens of both sexes. With the exception of PantUGT11 and PantUGT13 in the antennae, virtually all the genes could be detected in both antennae and abdomens. Over 70% of the genes (25/34) were abundantly transcribed in female and/or male abdomens. Among these, 8 genes exhibited significantly higher expression in female abdomens compared to males (PantUGT2/6/11/13/14/20/30/34). In contrast, 6 relatives were sex-biased genes in male abdomens (PantUGT3/4/7/12/22/26/). In the antennae, 5 PantUGT genes had relatively high expression (PantUGT3/16/18/24/31). Of these, PantUGT3 had male-biased expression, while PantUGT16, UGT18 and UGT31 were female-biased transcripts. The remaining 4 genes (i.e., PantUGT5/8/26/32) presented abundant expression in the antennae and abdomens of both sexes (Figure 4).

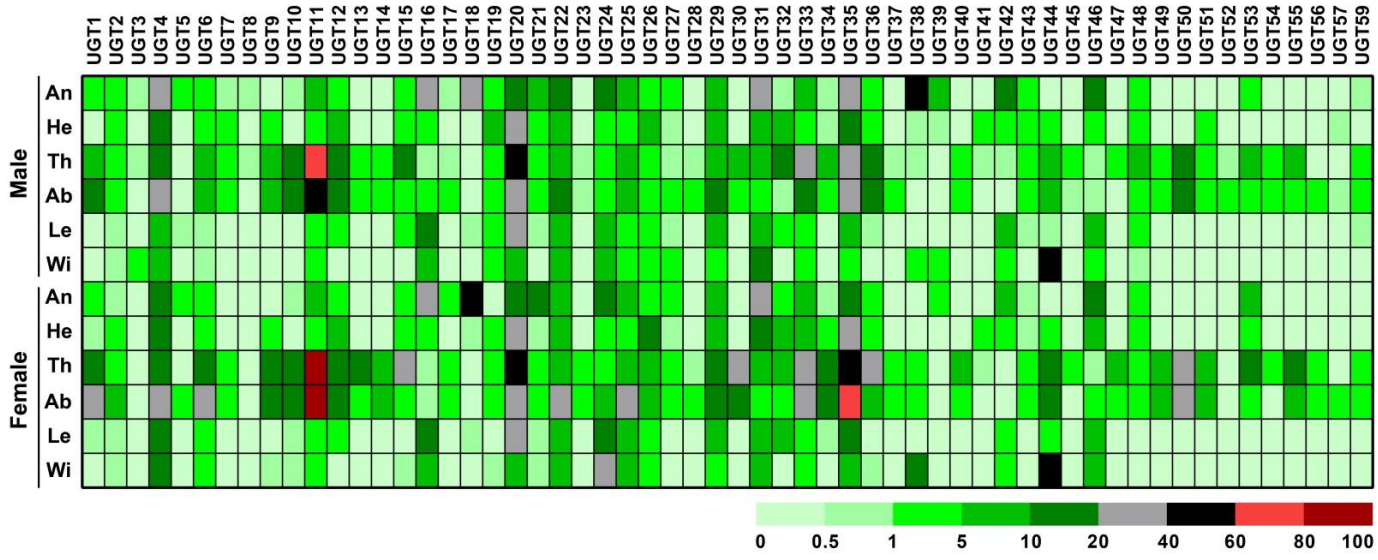

(**A**)

Figure 3. *Cont.*

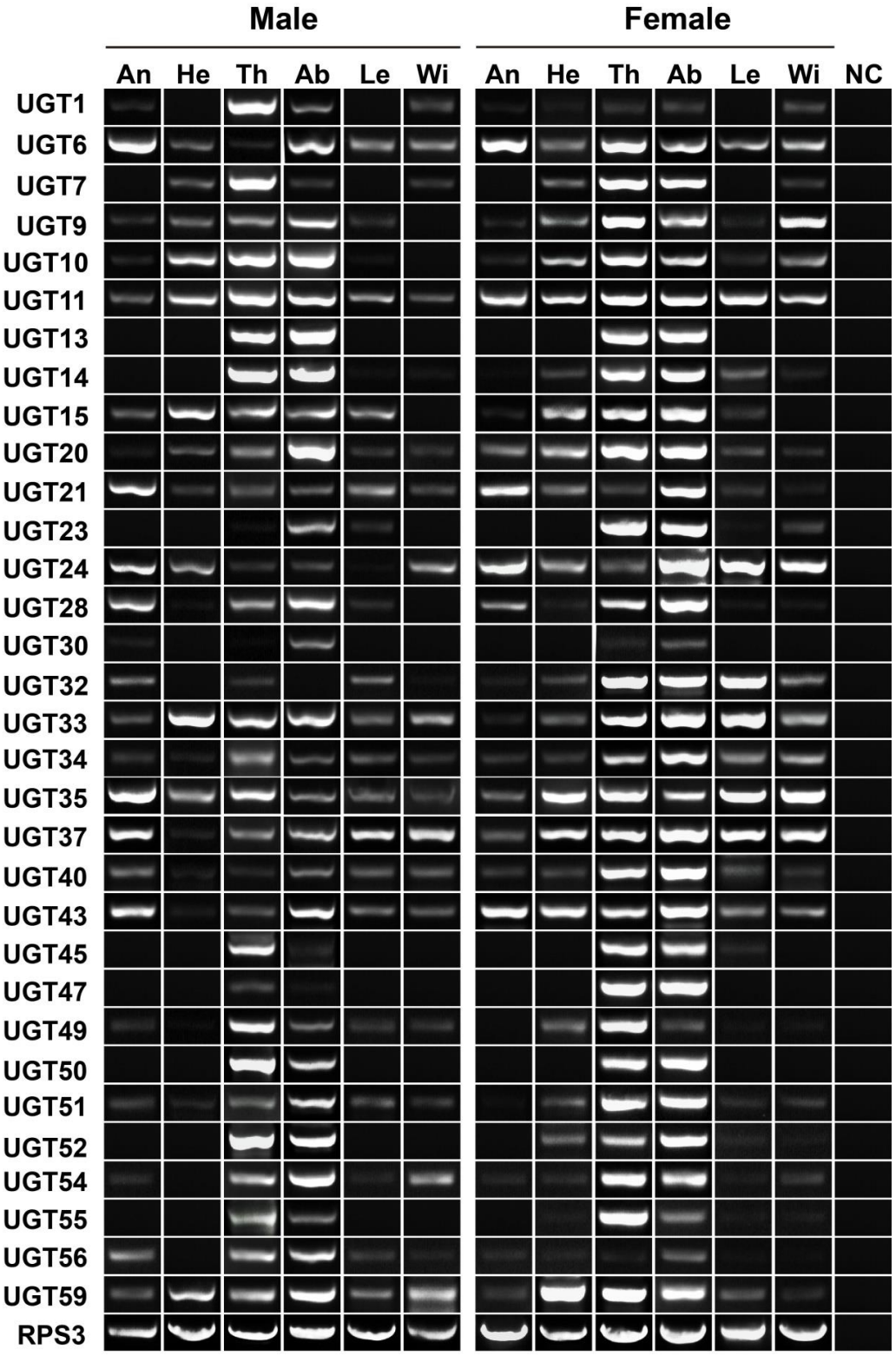

(**B**)

Figure 3. Expression pattern of candidate UGT genes in different tissues of *P. antennata*. (**A**) Expression patterns of PantUGT genes with FPKM values. (**B**) Expression patterns of PantUGT genes with PCR assays. PantRPS3 was used as the reference gene to detect the quality and quantity of cDNA templates. An: antennae; He: heads without antennae; Th: thoraxes; Ab: abdomens; Le: legs; Wi: wings; NC: negative control using sterile water as the template.

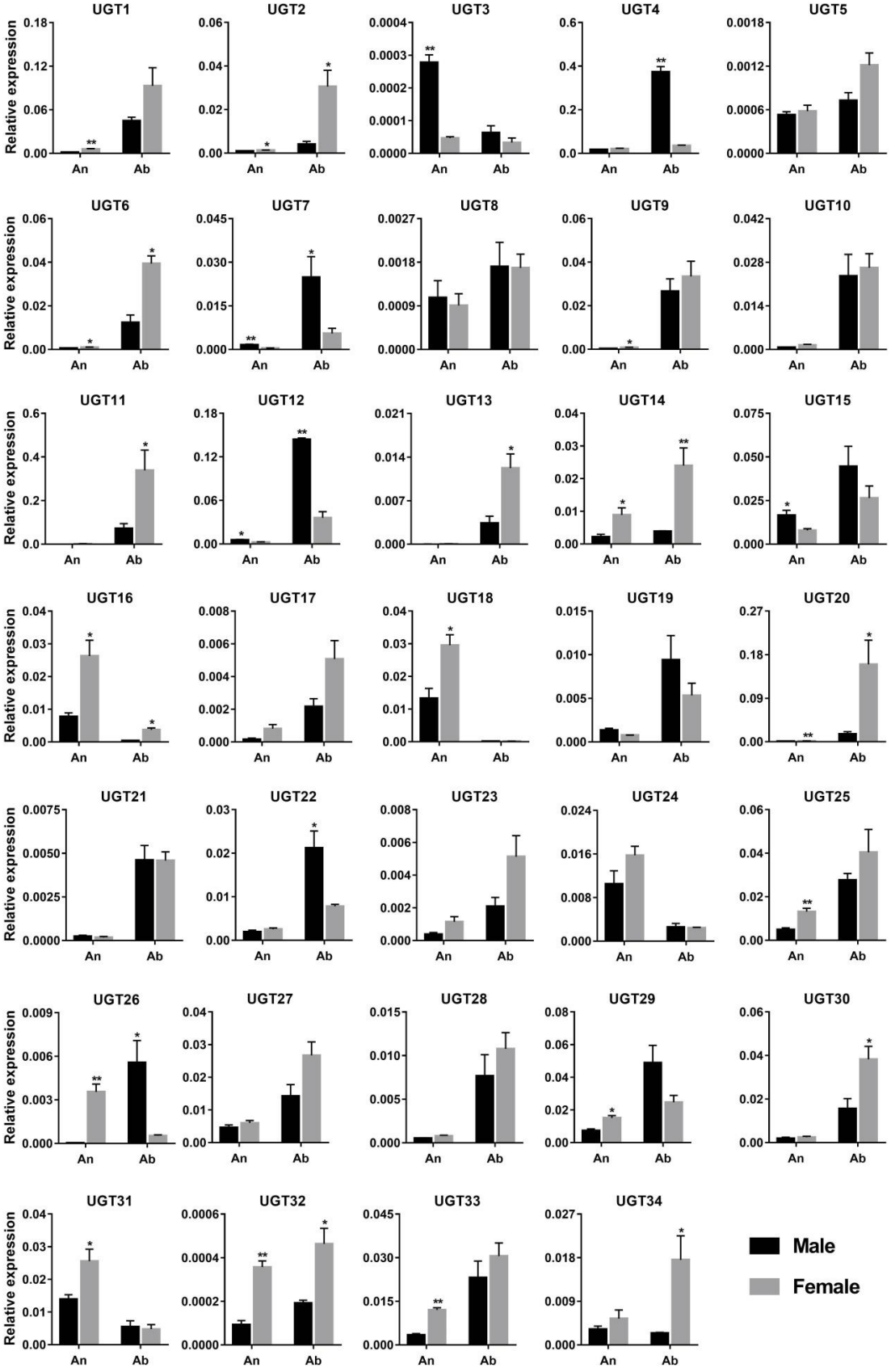

Figure 4. qPCR analysis of 34 UGT genes in antennae (An) and abdomens (Ab) of both sexes from *P. antennata*. Error bars represent the standard errors of three biological replicates. Asterisks denote significant differences in gene expression levels between female and male tissues (* $p < 0.05$, ** $p < 0.01$).

3.5. Candidate P. antennata UGTs Involved in Olfaction

With a focus on the olfactory roles of PantUGTs, we aimed to identify candidates expressed in the antennae. Based on the transcriptome data (FPKM > 1) and PCR results, the expression of 48 PantUGT genes was detectable. In the qPCR analyses, 32 out of 34 genes were expressed in the antennae, 9 of which had relatively high levels (PantUGT4/15/16/18/24/25/29/31/33) (Figure 4). In the remaining 25 PantUGTs, the FPKM values of 9 genes were above 1. It is worth noting that although the other 16 genes had low transcriptional levels (FPKM < 1), 7 of them (PantUGT37/40/49/51/54/56/59) were found to have expression by RT–PCR (Figure 3).

4. Discussion

To adapt to their habitats and feeding host plants, the cerambycid beetles utilize UGT enzymes to metabolize a variety of xenobiotics, including plant defensive compounds and insecticides [8,43–45]. Our study characterized this UGT gene repertoire in *P. antennata*, a wood-boring pest. As indicated in previous studies, the UGT sizes in insects were associated with their host plant range [28,46]. Our current study identified as many as 59 UGT candidates from *P. antennata*, close to the number in the two generalist herbivores *A. glabripennis* (65 relatives) [28] and *Locusta migratoria* Linnaeus, 1758 (Orthoptera: Acrididae) (68 relatives) [46], but more than those in *R. horsfieldi* (36 UGTs) [29], *X. quadripes* (30 UGTs) [14] and *H. parallela* (20 UGTs) [15]. This is likely to reflect a wide range of host plants used by *P. antennata*, although to date there is a restricted record of hosts, as this beetle is found only on the Juglandaceae plants [32]. For other beetles with a broad range of hosts, their relatively fewer UGTs could possibly be attributed to the numbers of sequencing tissues, as cDNA libraries of 12 tissues in *P. antennata* were constructed and sequenced (SRA accession numbers SRX14711840–SRX14711851).

In the NCBI BLAST analyses, all the 59 PantUGTs could align well with the UGTs in *A. glabripennis*, suggesting a high degree of conservation of UGTs between the two beetles (>45% identities) [28]. This conservation was further supported by the 1:1 orthology between the two cerambycids, as observed in the tree (29 orthologous pairs). Although there was a low identity (31.78%) among *P. antennata* UGTs, high conservation of UGTs was found across coleopteran insects, especially in sugar donor binding sites and catalytic residues [8,14–16]. This may reflect, to some extent, conserved functions of insect UGTs. In previous studies, the UGT genes in one coleopteran species could form relatively individual clades in clusters, such as the seven clusters in *A. glabripennis* [28], four in *A. tumida*, *A. planipennis* and *T. castaneum*, three in *L. decemlineata* and two in *X. quadripes* and *H. parallela* [14,15]. In this study, when we used the UGTs from more coleopteran species to construct the tree, it was found that some species-specific expansions of UGTs disappeared, especially in Cerambycidae. Therefore, our current tree mainly presented the orthologous groups among four cerambycid species. In agreement with previous results, family-specific clusters were common in coleopteran UGTs [8,14]. Based on the numbers of UGTs in *A. glabripennis* (58 candidates excluding 7 pseudogenes) and the orthology of UGTs between *P. antennata* and *A. glabripennis* [28], our study is likely to have identified most, if not all, of this beetle's UGT genes.

Insect UGTs generally have a wide tissue expression profile, associated with functional diversities responsible for insecticide resistance [31,47–49], sclerotization [50,51], detoxification [12,13], olfaction [17,18,52,53], pigmentation [54], cold tolerance [55] and immunity [56,57]. Our study revealed a broad tissue expression profile, with the majority of PantUGTs exhibiting particularly high levels in thoraxes and/or abdomens. The expression features were consistent with the UGT results in *H. parallela* [15], *X. quadripes* [14] and *R. horsfieldi* [29], as well as non-coleopteran species such as *B. mori* [8,58], *D. melanogaster* [8,59] and *Athetis lepigone* Möschler, 1860 (Lepidoptera: Noctuidae) [16]. In several previous studies, the UGT genes were highly transcribed in tissues responsible for detoxification, including midguts, fat bodies and Malpighian tubules [8,58,59]. In *P. antennata*, at least

half of the UGTs were expressed predominantly in female or male abdomens. Thus, it is suggested that these UGTs in this beetle may be expressed in detoxification-related tissues.

Odorant degrading enzymes, comprising a few cytochrome P450s, esterases and glutathione-S-transferases, and aldehyde oxidases, are highly expressed in antennae, and are capable of degrading plant odorants, sex pheromones or insecticides [60–64]. Like these degrading enzymes, some UGT members display dominant expression in the antennae, with involvement in olfaction. In *D. melanogaster*, DmelUGT36E1 expressed in antennal olfactory sensory neurons responded to the sex pheromone 2-heptanone [52]. In *Spodoptera littoralis* Boisduval, 1833 (Lepidoptera: Noctuidae), two antenna-specific UGTs (SlitUGT40R3 and SlitUGT46A6) were involved in the degradation of *Z*3-hexenyl acetate, *Z*9,*E*11-tetradecadienyl acetate or deltamethrin, as their expression was significantly regulated by these chemicals [18]. In Coleoptera, although no direct functional evidence demonstrates the roles of UGTs in olfaction, the UGTs from several beetles have been suggested to have putative olfactory associations with a specific or high transcription in the antennae, including those from *H. parallela* [15], *X. quadripes* [14] and *R. horsfieldi* [29]. Our study identified a number of *P. antennata* UGTs from the antennae. Considering the importance of the antennae in the perception of semiochemicals, the species may encounter many plant defensive compounds or general odorants. Therefore, some detoxification-related enzymes such as UGTs are expressed in the antennae and are responsible for the detoxification and removal of these chemicals, as evidenced in moth species [12,13]. Meanwhile, some sex-biased UGT genes were found, possibly associated with specific physiological activities of *P. antennata* such as mate recognition and oviposition.

5. Conclusions

In summary, our study revealed a comparable UGT number in *P. antennata*, with the identification of 59 relatives from the transcriptome. This large UGT gene repertoire may reflect a broad range of host plants in this beetle. Sequence and phylogenetic analyses indicate a high degree of conservation among cerambycid UGTs, especially for key amino acids involved in catalysis and sugar donor binding. *P. antennata* UGTs are widely expressed in tissues, including the antennae and abdomens, with involvement in olfaction and detoxification. In particular, some sex-biased UGT genes are found in the antennae, possibly associated with odorant reception in specific olfactory behaviors of *P. antennata*.

Supplementary Materials: The following supporting information can be downloaded at: https://www.mdpi.com/article/10.3390/d14050348/s1. Table S1: Primers used for the expression profiling analyses of *PantUGT* genes from *P. antennata*; Additional File S1: Amino acid sequences of coleopteran UGTs in the phylogenetic tree.

Author Contributions: Conceptualization, N.L.; methodology, N.Y., Z.W. and H.X.; validation, N.Y. and Z.W.; investigation, N.Y., Z.W., H.X. and T.L.; resources, N.L. and Z.W.; data curation, N.Y. and N.L.; writing—original draft preparation, N.L. and N.Y.; writing—review and editing, N.L. and N.Y.; supervision, N.L.; project administration, N.L.; funding acquisition, N.L. All authors have read and agreed to the published version of the manuscript.

Funding: This work was supported by the Yunnan Fundamental Research Project (202001AT070100) and the Yunnan Provincial Support Plan for the Cultivation of High-level Talents (Young Top-notch Talents) (YNWR_ QNBJ_2019_057).

Institutional Review Board Statement: Not applicable.

Data Availability Statement: The transcriptome of *P. antennata* has been deposited in the NCBI Sequence Read Archive (SRA) under the accession numbers SRX14711840–SRX14711851.

Conflicts of Interest: The authors declare no conflict of interest.

References

1. Bruinsma, M.; Dicke, M. Herbivore-Induced Indirect Defense: From Induction Mechanisms to Community Ecology. In *Induced Plant Resistance to Herbivory*; Schaller, A., Ed.; Springer: Dordrecht, The Netherland, 2008; pp. 31–60.
2. Despres, L.; David, J.P.; Gallet, C. The evolutionary ecology of insect resistance to plant chemicals. *Trends Ecol. Evol.* **2007**, *22*, 298–307. [CrossRef] [PubMed]
3. Ferry, N.; Edwards, M.G.; Gatehouse, J.A.; Gatehouse, A.M. Plant-insect interactions: Molecular approaches to insect resistance. *Curr. Opin. Biotechnol.* **2004**, *15*, 155–161. [CrossRef] [PubMed]
4. Li, X.; Schuler, M.A.; Berenbaum, M.R. Molecular mechanisms of metabolic resistance to synthetic and natural xenobiotics. *Annu. Rev. Entomol.* **2007**, *52*, 231–253. [CrossRef] [PubMed]
5. Bock, K.W. Vertebrate UDP-glucuronosyltransferases: Functional and evolutionary aspects. *Biochem. Pharmacol.* **2003**, *66*, 691–696. [CrossRef]
6. Bock, K.W. The UDP-glycosyltransferase (UGT) superfamily expressed in humans, insects and plants: Animal-plant arms-race and co-evolution. *Biochem. Pharmacol.* **2016**, *99*, 11–17. [CrossRef] [PubMed]
7. Meech, R.; Hu, D.G.; McKinnon, R.A.; Mubarokah, S.N.; Haines, A.Z.; Nair, P.C.; Rowland, A.; Mackenzie, P.I. The UDP-Glycosyltransferase (UGT) Superfamily: New Members, New Functions, and Novel Paradigms. *Physiol. Rev.* **2019**, *99*, 1153–1222. [CrossRef]
8. Ahn, S.J.; Vogel, H.; Heckel, D.G. Comparative analysis of the UDP-glycosyltransferase multigene family in insects. *Insect Biochem. Mol. Biol.* **2012**, *42*, 133–147. [CrossRef]
9. Ahn, S.-J.; Chertemps, T.; Maïbèche, M.; Marygold, S.J.; Van Leeuwen, T. Editorial: Invertebrate UDP-Glycosyltransferases: Nomenclature, Diversity and Functions. *Front. Physiol.* **2021**, *12*, 748290. [CrossRef]
10. Daimon, T.; Hirayama, C.; Kanai, M.; Ruike, Y.; Meng, Y.; Kosegawa, E.; Nakamura, M.; Tsujimoto, G.; Katsuma, S.; Shimada, T. The silkworm *Green b* locus encodes a quercetin 5-O-glucosyltransferase that produces green cocoons with UV-shielding properties. *Proc. Natl. Acad. Sci. USA* **2010**, *107*, 11471–11476. [CrossRef]
11. Luque, T.; Okano, K.; O'Reilly, D.R. Characterization of a novel silkworm (*Bombyx mori*) phenol UDP-glucosyltransferase. *Eur. J. Biochem.* **2002**, *269*, 819–825. [CrossRef]
12. Krempl, C.; Sporer, T.; Reichelt, M.; Ahn, S.J.; Heidel-Fischer, H.; Vogel, H.; Heckel, D.G.; Joußen, N. Potential detoxification of gossypol by UDP-glycosyltransferases in the two Heliothine moth species *Helicoverpa armigera* and *Heliothis virescens*. *Insect Biochem. Mol. Biol.* **2016**, *71*, 49–57. [CrossRef] [PubMed]
13. Israni, B.; Wouters, F.C.; Luck, K.; Seibel, E.; Ahn, S.J.; Paetz, C.; Reinert, M.; Vogel, H.; Erb, M.; Heckel, D.G.; et al. The fall armyworm *Spodoptera frugiperda* utilizes specific UDP-glycosyltransferases to inactivate maize defensive benzoxazinoids. *Front. Physiol.* **2020**, *11*, 604754. [CrossRef] [PubMed]
14. Yin, N.N.; Zhao, Y.J.; Zhu, J.Y.; Liu, N.Y. Antennal UDP-glycosyltransferase genes in the coffee white stemborer, *Xylotrechus quadripes*. *J. Asia-Pac. Entomol.* **2019**, *22*, 1145–1153. [CrossRef]
15. Wang, S.; Liu, Y.; Zhou, J.J.; Yi, J.K.; Pan, Y.; Wang, J.; Zhang, X.X.; Wang, J.X.; Yang, S.; Xi, J.H. Identification and tissue expression profiling of candidate UDP-glycosyltransferase genes expressed in *Holotrichia parallela* motschulsky antennae. *B Entomol. Res.* **2018**, *108*, 807–816. [CrossRef]
16. Zhang, Y.N.; Ma, J.F.; Xu, L.; Dong, Z.P.; Xu, J.W.; Li, M.Y.; Zhu, X.Y. Identification and expression patterns of UDP-glycosyltransferase (UGT) genes from insect pest *Athetis lepigone* (Lepidoptera: Noctuidae). *J. Asia-Pac. Entomol.* **2017**, *20*, 253–259. [CrossRef]
17. Younus, F.; Chertemps, T.; Pearce, S.L.; Pandey, G.; Bozzolan, F.; Coppin, C.W.; Russell, R.J.; Maibeche-Coisne, M.; Oakeshott, J.G. Identification of candidate odorant degrading gene/enzyme systems in the antennal transcriptome of *Drosophila melanogaster*. *Insect Biochem. Mol. Biol.* **2014**, *53*, 30–43. [CrossRef]
18. Bozzolan, F.; Siaussat, D.; Maria, A.; Durand, N.; Pottier, M.A.; Chertemps, T.; Maibeche-Coisne, M. Antennal uridine diphosphate (UDP)-glycosyltransferases in a pest insect: Diversity and putative function in odorant and xenobiotics clearance. *Insect Mol. Biol.* **2014**, *23*, 539–549. [CrossRef]
19. Wang, Q.; Hasan, G.; Pikielny, C.W. Preferential expression of biotransformation enzymes in the olfactory organs of *Drosophila melanogaster*, the antennae. *J. Biol. Chem.* **1999**, *274*, 10309–10315. [CrossRef]
20. Chen, X.; Xia, J.; Shang, Q.; Song, D.; Gao, X. UDP-glucosyltransferases potentially contribute to imidacloprid resistance in *Aphis gossypii* glover based on transcriptomic and proteomic analyses. *Pestic. Biochem. Physiol.* **2019**, *159*, 98–106. [CrossRef]
21. Pan, Y.; Wen, S.; Chen, X.; Gao, X.; Zeng, X.; Liu, X.; Tian, F.; Shang, Q. UDP-glycosyltransferases contribute to spirotetramat resistance in *Aphis gossypii* Glover. *Pestic. Biochem. Physiol.* **2020**, *166*, 104565. [CrossRef]
22. Yang, N.; Xie, W.; Yang, X.; Wang, S.; Wu, Q.; Li, R.; Pan, H.; Liu, B.; Shi, X.; Fang, Y.; et al. Transcriptomic and proteomic responses of sweetpotato whitefly, *Bemisia tabaci*, to thiamethoxam. *PLoS ONE* **2013**, *8*, e61820. [CrossRef] [PubMed]
23. Tian, F.; Wang, Z.; Li, C.; Liu, J.; Zeng, X. UDP-Glycosyltransferases are involved in imidacloprid resistance in the Asian citrus psyllid, *Diaphorina citri* (Hemiptera: Lividae). *Pestic. Biochem. Physiol.* **2019**, *154*, 23–31. [CrossRef] [PubMed]
24. Zhou, Y.; Fu, W.B.; Si, F.L.; Yan, Z.T.; Zhang, Y.J.; He, Q.Y.; Chen, B. UDP-glycosyltransferase genes and their association and mutations associated with pyrethroid resistance in *Anopheles sinensis* (Diptera: Culicidae). *Malar. J.* **2019**, *18*, 62. [CrossRef]
25. Pedra, J.H.F.; McIntyre, L.M.; Scharf, M.E.; Pittendrigh, B.R. Genome-wide transcription profile of field- and laboratory-selected dichlorodiphenyltrichloroethane (DDT)-resistant *Drosophila*. *Proc. Natl. Acad. Sci. USA* **2004**, *101*, 7034–7039. [CrossRef] [PubMed]

26. Vontas, J.; Blass, C.; Koutsos, A.C.; David, J.P.; Kafatos, F.C.; Louis, C.; Hemingway, J.; Christophides, G.K.; Ranson, H. Gene expression in insecticide resistant and susceptible *Anopheles gambiae* strains constitutively or after insecticide exposure. *Insect Mol. Biol.* **2005**, *14*, 509–521. [CrossRef]
27. Li, X.; Zhu, B.; Gao, X.; Liang, P. Over-expression of UDP-glycosyltransferase gene UGT2B17 is involved in chlorantraniliprole resistance in *Plutella xylostella* (L.). *Pest Manag. Sci.* **2017**, *73*, 1402–1409. [CrossRef] [PubMed]
28. McKenna, D.D.; Scully, E.D.; Pauchet, Y.; Hoover, K.; Kirsch, R.; Geib, S.M.; Mitchell, R.F.; Waterhouse, R.M.; Ahn, S.J.; Arsala, D.; et al. Genome of the Asian longhorned beetle (*Anoplophora glabripennis*), a globally significant invasive species, reveals key functional and evolutionary innovations at the beetle-plant interface. *Genome Biol.* **2016**, *17*, 227. [CrossRef]
29. Wang, Z.Q.; Yin, N.N.; Zhao, N.; Liu, N.Y. Identification and expression characterization of UDP-glucosyltransferase genes in *Rhaphuma horsfieldi*. *Chin. J. Appl. Entomol.* **2020**, *57*, 898–910.
30. Wu, Z.; Bin, S.; He, H.; Wang, Z.; Li, M.; Lin, J. Differential expression analysis of chemoreception genes in the striped flea beetle *Phyllotreta striolata* using a transcriptomic approach. *PLoS ONE* **2016**, *11*, e0153067. [CrossRef]
31. Kaplanoglu, E.; Chapman, P.; Scott, I.M.; Donly, C. Overexpression of a cytochrome P450 and a UDP-glycosyltransferase is associated with imidacloprid resistance in the Colorado potato beetle, *Leptinotarsa decemlineata*. *Sci. Rep.* **2017**, *7*, 1762. [CrossRef]
32. Yin, N.N.; Zhao, Y.J.; Zhao, N.; Liu, N.Y. Morphological characteristics of *Pharsalia antennata* and its sensilla ultrastructure. *Plant. Protection.* **2020**, *46*, 30–40.
33. Hall, T.A. BioEdit: A User-Friendly Biological Sequence Alignment Editor and Analysis Program for Windows 95/98/NT. *Nucleic Acids Symp. Ser.* **1999**, *41*, 95–98.
34. Nicholas, K.B.; Nicholas, H.B.; Deerfield, D.W. GeneDoc: Analysis and visualization of genetic variation. *EMBNEW News* **1997**, *4*, 14.
35. Teufel, F.; Almagro Armenteros, J.J.; Johansen, A.R.; Gíslason, M.H.; Pihl, S.I.; Tsirigos, K.D.; Winther, O.; Brunak, S.; von Heijne, G.; Nielsen, H. SignalP 6.0 predicts all five types of signal peptides using protein language models. *Nat. Biotechnol.* **2022**. [CrossRef]
36. Katoh, K.; Standley, D.M. MAFFT multiple sequence alignment software version 7: Improvements in performance and usability. *Mol. Biol. Evol.* **2013**, *30*, 772–780. [CrossRef]
37. Price, M.N.; Dehal, P.S.; Arkin, A.P. FastTree 2—Approximately maximum-likelihood trees for large alignments. *PLoS ONE.* **2010**, *5*, e9490. [CrossRef]
38. Trapnell, C.; Williams, B.A.; Pertea, G.; Mortazavi, A.; Kwan, G.; van Baren, M.J.; Salzberg, S.L.; Wold, B.J.; Pachter, L. Transcript assembly and quantification by RNA-Seq reveals unannotated transcripts and isoform switching during cell differentiation. *Nat. Biotechnol.* **2010**, *28*, 511–515. [CrossRef]
39. Simon, P. Q-Gene: Processing quantitative real-time RT-PCR data. *Bioinformatics* **2003**, *19*, 1439–1440. [CrossRef]
40. Muller, P.Y.; Janovjak, H.; Miserez, A.R.; Dobbie, Z. Processing of gene expression data generated by quantitative real-time RT-PCR. *BioTechniques* **2002**, *32*, 1372–1374, 1376, 1378–1379.
41. Miley, M.J.; Zielinska, A.K.; Keenan, J.E.; Bratton, S.M.; Radominska-Pandya, A.; Redinbo, M.R. Crystal structure of the cofactor-binding domain of the human phase II drug-metabolism enzyme UDP-glucuronosyltransferase 2B7. *J. Mol. Biol.* **2007**, *369*, 498–511. [CrossRef]
42. Waterhouse, A.; Bertoni, M.; Bienert, S.; Studer, G.; Tauriello, G.; Gumienny, R.; Heer, F.T.; de Beer, T.A.P.; Rempfer, C.; Bordoli, L.; et al. SWISS-MODEL: Homology modelling of protein structures and complexes. *Nucleic Acids Res.* **2018**, *46*, W296–W303. [CrossRef] [PubMed]
43. Allison, J.D.; Borden, J.H.; Seybold, S.J. A review of the chemical ecology of the Cerambycidae (Coleoptera). *Chemoecology* **2004**, *14*, 123–150. [CrossRef]
44. Trowbridge, A.M. Evolutionary ecology of chemically mediated plant-insect interactions. In *Ecology and the Environment*; Monson, R.K., Ed.; Springer: New York, NY, USA, 2014; pp. 1–28.
45. Nagare, M.; Ayachit, M.; Agnihotri, A.; Schwab, W.; Joshi, R. Glycosyltransferases: The multifaceted enzymatic regulator in insects. *Insect Mol. Biol.* **2021**, *30*, 123–137. [CrossRef]
46. Wang, X.; Fang, X.; Yang, P.; Jiang, X.; Jiang, F.; Zhao, D.; Li, B.; Cui, F.; Wei, J.; Ma, C.; et al. The locust genome provides insight into swarm formation and long-distance flight. *Nat. Commun.* **2014**, *5*, 2957. [CrossRef] [PubMed]
47. Hu, B.; Zhang, S.H.; Ren, M.M.; Tian, X.R.; Wei, Q.; Mburu, D.K.; Su, J.Y. The expression of *Spodoptera exigua* P450 and UGT genes: Tissue specificity and response to insecticides. *Insect Sci.* **2019**, *26*, 199–216.
48. Li, X.; Shi, H.; Gao, X.; Liang, P. Characterization of UDP-glucuronosyltransferase genes and their possible roles in multi-insecticide resistance in *Plutella xylostella* (L.). *Pest. Manag. Sci.* **2018**, *74*, 695–704. [CrossRef]
49. Chen, X.; Tang, C.; Ma, K.; Xia, J.; Song, D.; Gao, X.W. Overexpression of UDP-glycosyltransferase potentially involved in insecticide resistance in *Aphis gossypii* Glover collected from Bt cotton fields in China. *Pest. Manag. Sci.* **2020**, *76*, 1371–1377. [CrossRef]
50. Hopkins, T.L.a.; Kramer, K.J. Insect Cuticle Sclerotization. *Annu.Rev. Entomol.* **1992**, *37*, 273–302. [CrossRef]
51. Kramer, K.J.; Hopkins, T.L. Tyrosine metabolism for insect cuticle tanning. *Arch. Insect Biochem. Physiol.* **1987**, *6*, 279–301.
52. Fraichard, S.; Legendre, A.; Lucas, P.; Chauvel, I.; Faure, P.; Neiers, F.; Artur, Y.; Briand, L.; Ferveur, J.F.; Heydel, J.M. Modulation of sex pheromone discrimination by a UDP-glycosyltransferase in *Drosophila melanogaster*. *Genes* **2020**, *11*, 237. [CrossRef]

53. He, P.; Zhang, Y.F.; Hong, D.Y.; Wang, J.; Wang, X.L.; Zuo, L.H.; Tang, X.F.; Xu, W.-M.; He, M. A reference gene set for sex pheromone biosynthesis and degradation genes from the diamondback moth, *Plutella xylostella*, based on genome and transcriptome digital gene expression analyses. *BMC Genomics* **2017**, *18*, 219. [CrossRef] [PubMed]
54. Wiesen, B.; Krug, E.; Fiedler, K.; Wray, V.; Proksch, P. Sequestration of host-plant-derived flavonoids by lycaenid butterfly *Polyommatus icarus*. *J. Chem. Ecol.* **1994**, *20*, 2523–2538. [CrossRef] [PubMed]
55. Königer, A.; Grath, S. Transcriptome analysis reveals candidate genes for cold tolerance in *Drosophila* ananassae. *Genes* **2018**, *9*, 624. [CrossRef] [PubMed]
56. Kimbrell, D.A.; Hice, C.; Bolduc, C.; Kleinhesselink, K.; Beckingham, K. The Dorothy enhancer has tinman binding sites and drives hopscotch-induced tumor formation. *Genesis* **2002**, *34*, 23–28. [CrossRef]
57. Zhou, Z.; Rodriguez, A.; Wu, C.Y.; Kimbrell, D.A. *Drosophila* cellular immune system: Dorothy encodes a UDP glycosyltransferase. *Adv. Exp. Med. Biol.* **2001**, *484*, 251–263.
58. Huang, F.F.; Chai, C.L.; Zhang, Z.; Liu, Z.H.; Dai, F.Y.; Lu, C.; Xiang, Z.H. The UDP-glucosyltransferase multigene family in *Bombyx mori*. *BMC Genomics* **2008**, *9*, 563. [CrossRef]
59. Ahn, S.-J.; Marygold, S.J. The UDP-glycosyltransferase family in *Drosophila melanogaster*: Nomenclature update, gene expression and phylogenetic analysis. *Front. Physiol.* **2021**, *12*, 648481. [CrossRef]
60. Durand, N.; Carot-Sans, G.; Bozzolan, F.; Rosell, G.; Siaussat, D.; Debernard, S.; Chertemps, T.; Maibeche-Coisne, M. Degradation of pheromone and plant volatile components by a same odorant-degrading enzyme in the cotton leafworm, *Spodoptera littoralis*. *PLoS ONE* **2011**, *6*, e29147. [CrossRef]
61. Godoy, R.; Machuca, J.; Venthur, H.; Quiroz, A.; Mutis, A. An overview of antennal esterases in Lepidoptera. *Front. Physiol.* **2021**, *12*, 643281. [CrossRef]
62. Xu, W.; Liao, Y. Identification and characterization of aldehyde oxidases (AOXs) in the cotton bollworm. *Naturwissenschaften* **2017**, *104*, 94. [CrossRef]
63. Liu, H.; Tang, Y.; Wang, Q.; Shi, H.; Yin, J.; Li, C. Identification and characterization of an antennae-specific glutathione S-transferase from the Indian meal moth. *Front. Physiol.* **2021**, *12*, 727619. [CrossRef] [PubMed]
64. Feyereisen, R. Evolution of insect P450. *Biochem. Soc. Trans.* **2006**, *34*, 1252–1255. [CrossRef] [PubMed]